



HAL
open science

Degradation of diatom carbohydrates: A case study with N- and Si-stressed *Thalassiosira weissflogii*

Maxime Suroy, Christos Panagiotopoulos, Julia Boutorh, M. Goutx, Brivaëla
Moriceau

► To cite this version:

Maxime Suroy, Christos Panagiotopoulos, Julia Boutorh, M. Goutx, Brivaëla Moriceau. Degradation of diatom carbohydrates: A case study with N- and Si-stressed *Thalassiosira weissflogii*. *Journal of Experimental Marine Biology and Ecology*, 2015, 470, pp.1-11. 10.1016/j.jembe.2015.04.018 . hal-03622281v1

HAL Id: hal-03622281

<https://hal.science/hal-03622281v1>

Submitted on 29 Mar 2022 (v1), last revised 13 Dec 2023 (v2)

HAL is a multi-disciplinary open access archive for the deposit and dissemination of scientific research documents, whether they are published or not. The documents may come from teaching and research institutions in France or abroad, or from public or private research centers.

L'archive ouverte pluridisciplinaire **HAL**, est destinée au dépôt et à la diffusion de documents scientifiques de niveau recherche, publiés ou non, émanant des établissements d'enseignement et de recherche français ou étrangers, des laboratoires publics ou privés.

1 Degradation of diatom carbohydrates: A case study with N- and Si-
2 stressed *Thalassiosira weissflogii*

3
4
5 Maxime Suroy^a, Christos Panagiotopoulos^{a*}, Julia Boutorh^b, Madeleine Goutx^a and Brivaëla
6 Moriceau^b

7
8
9 ^a Aix Marseille Université, CNRS/INSU, Université de Toulon, IRD, Mediterranean Institute of
10 Oceanography (MIO) UM 110, 13288, Marseille, France

11 ^b Université de Brest, Institut Universitaire Européen de la Mer (IUEM), CNRS, Laboratoire
12 des Sciences de l'Environnement Marin, UMR 6539 CNRS/UBO/IFREMER/IRD, 29280
13 Plouzané, France
14
15
16
17
18
19
20
21
22
23
24
25
26
27

28 *Corresponding author e-mail: christos.panagiotopoulos@mio.osupytheas.fr

29
30 Journal of Experimental Marine Biology and Ecology

31
32 Accepted version

33
34 20 April 2015

39 **Abstract**

40 Diatoms are a key phytoplanktonic group that affects the carbon cycle in the ocean. Although
41 the effect of nutrient limitation on the primary productivity of diatoms is well-studied, the
42 effect of such a limitation on the organic matter quality of diatoms and their vertical transport
43 through the water column remains unclear. In this study, the diatom *Thalassiosira weissflogii*
44 (TW) was grown under two different nutrient conditions, ‘N-stress’ and ‘Si-stress’, and was
45 compared against healthy TW cells (Nutrient-replete). Biodegradation experiments of TW
46 were performed for all of the above conditions, and the particulate fraction was monitored
47 over time (~ one month) in terms of the organic carbon (POC), nitrogen (PON), and sugars
48 (PCHO), including prokaryotic counting. Using these results, we estimated the degradation
49 rate constants for POC, PON, PCHO, and the individual carbohydrate monomers
50 (monosaccharides) for the TW cells. Our results indicated that the N- and Si-limitations
51 increase the organic carbon content of the TW cells with a concomitant decrease in the silicon
52 content (bSiO₂), suggesting a modification of the TW cells. The PCHO content increased by a
53 factor of 2.6 and 3.8 in the N-stress and Si-stress cells, respectively. At the beginning of the
54 experiment (T₀), the N-stress and Si-stress cells were characterized by higher amounts of
55 glucose (5-32 mol%) and xylose (13-19 mol%), compared with the Nutrient-replete cells,
56 which were dominated by ribose (~22 mol%), indicating differences in the physiological
57 status of the TW cells and/or in the synthesis of storage/structural polysaccharides. The first
58 order degradation rate constants (k_1) for the POC were similar in all of the experiments (k_1 =
59 0.096-0.113 d⁻¹), which was not the case for the PON in which the highest values (by a factor
60 of ~2.5) were observed for the nutrient-replete experiment. This result indicates a different
61 behavior in the utilization and/or accessibility to prokaryotes of carbon and nitrogen during
62 the biodegradation experiment. Moreover, ribose, glucose, and galactose exhibited the highest
63 degradation rate constants in all of the experiments, which further reflects the differences in

64 their initial macromolecular origin (*e.g.*, storage vs structural carbohydrates) and highlights
65 the changes in the organic matter quality during growth under nutrient-limited conditions and
66 degradation. These results suggest that the ‘nutrient-stress’ diatoms may affect the export of
67 carbon (particularly carbohydrates) relative to nitrogen in the ocean interior compared with
68 the diatoms grown under optimal conditions.

69

70 Keywords :*Thalassiosira weissflogii*, biodegradation experiment, carbohydrates, N- and Si-
71 limitation, degradation rate constants

72 **1. Introduction**

73 Diatoms are a key phytoplanktonic group responsible for nearly 25 to 35% of the total
74 primary production in oceans (Aumont et al., 2003; Nelson et al., 1995; Uitz et al., 2010).
75 Moreover, diatoms are important contributors to organic carbon export because they are often
76 associated with the formation of large aggregates made of fresh material or phytodetritus that
77 rapidly sink to the ocean interior, with sinking velocities averaging $\sim 100 \text{ m d}^{-1}$ (Goutx et al.,
78 2007; Martin et al., 2011; Sarthou et al., 2005). Finally, diatoms form most of the
79 sedimentation fluxes along with coccolitophores (Engel et al. 2009) and large fecal pellets
80 (Thornton, 2002; Turner, 2002); therefore, they considerably influence the functioning of the
81 biological carbon pump (Buesseler, 1998; Volk and Hoffert, 1985).

82 The efficiency of the diatoms to export organic carbon to the ocean interior depends
83 not only on their productivity, but also on the balance between the sinking velocity of the
84 particles and their degradation rates, both of which are controlled by biotic and abiotic
85 parameters. These parameters include aggregation/disaggregation rates of the particles (Logan
86 et al., 1995), particle size/density (De La Rocha and Passow, 2007 and references therein), the
87 prokaryotic community attached to the particles (Legendre and Rivkin, 2002), temperature
88 (Bidle et al., 2002; Iversen and Ploug, 2013), pressure (Tamburini et al., 2006), and the
89 presence of minerals (Engel et al., 2009; Honda and Watanabe, 2010; Moriceau et al., 2009).

90 Nutrient limitations are known to affect the production of diatoms; however,
91 significantly less is known about their effect on diatom export. Nitrogen and silicon are the
92 two major nutrients limiting diatom productivity in the open ocean (Moore et al., 2002).
93 Nitrogen is considered to be the main element controlling primary marine production in the
94 ocean, whereas silicon is only required for silicified species, such as diatoms (Falkowski,
95 1997). Nutrient availability acts on the sinking velocities of a diatom by inducing biochemical
96 composition changes that can modify the organic matter (OM) quality and the cell buoyancy

97 (Lynn et al., 2000; Richardson and Cullen, 1995; Shifrin and Chisholm, 1981). Nitrogen and
98 silicon limitation generally results in a decrease in the growth rate of diatoms (Claquin et al.,
99 2002; Martin-Jézéquel et al., 2000), the nutrient uptake (De La Rocha et al., 2010), and a
100 decrease in the free amino acid and protein content (Martin-Jézéquel et al., 2000; Palmucci et
101 al., 2011). The modulation of the cell cycle involving these limitations also affects the frustule
102 silicification (Claquin et al., 2002; Martin-Jézéquel et al., 2000). Generally, frustules of
103 nitrogen-limited diatoms are thicker than those of silicon-limited diatoms due to a longer cell
104 cycle, which further indicates a decoupling between the silicon and nitrogen metabolisms
105 (Claquin et al., 2002; Hildebrand, 2002).

106 Although the effect of nutrient limitation on the biochemical composition of diatoms
107 cannot be generalized because of their different specific responses (Palmucci et al., 2011;
108 Shifrin and Chisholm, 1981), generally the decrease in growth rate results in a decrease in the
109 protein synthesis, which is compensated by an increase in storage compounds (e.g.,
110 carbohydrates). For example, nitrogen starvation results in an accumulation of carbohydrates
111 and a decrease in lipids (Shifrin and Chisholm, 1981; Suroy et al., 2014) in TW, an important
112 diatom species that dominates phytoplankton blooms after a nutrient input in certain oceanic
113 areas (Smetacek, 1985; Sorhannus et al., 2010). Although a significant number of studies has
114 focused on the degradation of particles and/or diatoms by following their bulk individual
115 components (e.g. proteins, carbohydrates, lipids, etc.; Harvey et al., 1995; Panagiotopoulos et
116 al. 2002), very few data currently exist at the molecular level regarding the above compound
117 classes (Harvey and Macko, 1997; Goutx et al., 2007) and especially those of carbohydrates.

118 To the best of our knowledge only the dynamics of amino acids have been explored
119 during the decomposition of calcifying and non-calcifying *Emiliania huxleyi* cultures (Engel
120 et al. 2009), whereas very little information exists on carbohydrates. Although carbohydrates
121 are less abundant in diatoms (~ 5-10% of their total dry weight; Brown et al., 1997) compared

122 with amino acids, they are among the most abundant compounds in particulate (5-15%;
123 Hernes et al., 1996; Panagiotopoulos and Sempéré, 2005a) and dissolved organic matter (2-
124 10%; Panagiotopoulos and Sempéré, 2005b and references therein).

125 The present study aims to explore the carbohydrate changes at the molecular level of
126 the diatom cells under variable environmental growth conditions and particularly assess the
127 effect of nutrient stress during biotic degradation. We used *Thalassiosira weissflogii* (TW) as
128 a model diatom and we tested the effect of two different nutrient stress conditions (nitrogen
129 and silicon starvations) on its carbohydrates composition. Degradation of nutrient-stress algae
130 was monitored over time (30 days), and the degradation rate constants of the individual
131 monosaccharides were estimated. The results are compared and discussed along with the bulk
132 degradation features of the particulate organic carbon and nitrogen.

133

134 **2. Materials and Methods**

135 **2.1 Experimental design**

136 The experimental protocol consisted of the production of TW cells which were grown
137 in three different conditions namely: ‘Nutrient-replete’, ‘N-stress’, and ‘Si-stress’ followed by
138 a degradation experiment (Fig.1). As such, the above TW cells were incubated in the darkness
139 with the presence of a natural prokaryote community.

140 “*Nutrient-replete*” and “*Nutrient-stress*” cultures. TW was grown in Conway
141 medium (Walne, 1966) in a large volume container culture at the Argenton Ifremer station at
142 20 °C under a 12 h:12 h light : dark cycle and an irradiance of 241 $\mu\text{mol photons m}^{-2} \text{s}^{-1}$. A
143 volume (10 L) of culture at a cell concentration of $4.0 \pm 0.26 \times 10^8 \text{ cell L}^{-1}$ was centrifuged
144 and the produced pellet was stored in the freezer (-20 °C) for one week. This material
145 corresponded to the “Nutrient-replete” cells. An additional volume of 20 L was equally
146 divided into two aliquots (Table 1). The cells were centrifuged, rinsed with artificial seawater

147 and resuspended in two container cultures filled with f/2 medium, NO_3^- and H_4SiO_4 free, for
148 the N-stress and Si-stress experiments, respectively. Because of laboratory logistical
149 constraints, “Nutrient-replete” and “Nutrient-stress” cells were produced in different growth
150 media (Conway medium vs f/2 medium). Previous studies showed little difference in the
151 diatom growth between f/2 and Conway media (Lahanan et al., 2013); therefore we may
152 confidently consider that the growth of TW in the Conway medium is representative of our
153 “Nutrient-replete” cells and comparable to the “Nutrient-stress” cultures.

154 The ‘N-stress’ and ‘Si-stress’ diatom container cultures were placed at 18 °C in a
155 growth chamber under a 12 h:12 h light : dark cycle at an irradiance of 158 $\mu\text{mol photons m}^{-2}$
156 s^{-1} for one week. The silicic acid (dSi), pH, nitrates, and phosphates were measured over time
157 to control the growth conditions of the cells (Boutorh et al *comm. pers.*). For the ‘N-stress’
158 culture, the nitrate concentrations were below the detection limit immediately after the
159 beginning of the starvation procedure, indicating an efficient starvation. Similarly, during the
160 Si-starvation experiment, the dSi concentrations ranged from 0 to 3.4 μM . The low dSi
161 concentrations were likely due to the dissolution of a certain amount of dead cells, but the
162 diatom still underwent Si-starvation (Sarhou et al., 2005). Moreover, during the Si-starvation,
163 the pH concentrations increased over time and reached values > 9.3 after day 6, indicating a
164 C-limitation. This pattern was not observed in the ‘N-stress’ culture in which the dSi
165 concentrations decreased over time to reach values $< 3.0 \mu\text{M}$ at day 6, indicating a late Si-
166 limitation. Similar to the above procedure, after one week of growth, the diatoms were
167 concentrated by centrifugation and killed by freezing at -20 °C. This was confirmed by flow
168 cytometry which showed that about 98% of the TW were killed at -20°C, while the cell
169 integrity was not disrupted (Soler, 2010).

170 *Degradation experiments.* The TW cells (‘Nutrient-replete’, ‘N-stress’, and ‘Si-stress’)
171 were resuspended in 10 L degradation batches, filled with 0.8 μm filtered natural seawater

172 sampled at a 10 m depth in the Bay of Brest (4° 33' 07.19 W, 48° 21' 32.13 N) in October
173 2011 (Fig.1). The physical and chemical hydrological characteristics of the area are provided
174 at the following link: <http://somlit.epoc.u-bordeaux1.fr/fr/>. The seawater was filtered on 0.8-
175 µm polycarbonate membrane (Millipore) to remove the phyto- and zooplanktonic organisms
176 while maintaining most of the natural prokaryotic community (Duhamel et al., 2007).
177 Epifluorescence microscopy analysis of the 0.8 µm filtrate revealed the presence of the
178 autochthonous prokaryotic community and very few picoeucaryotes cells (results not shown)
179 which agrees with previous studies (Duhamel et al., 2007).

180 The degradation batches were placed on an orbital shaker table at 16 °C in the dark,
181 and punched caps were used to ensure gas exchange. The batches were sampled for the
182 biochemical parameters (POC, PON, and PCHO), including the total count of the
183 heterotrophic prokaryotes over 30 days. Prior to each sampling, the batches were vigorously
184 shaken to ensure homogeneity. At the end of the degradation experiment, more than the half
185 of the initial volume remained (~6 L) in the bottle to reduce the experimental errors related to
186 the sample amounts. The number of replicates for each parameter (POC, PON, and PCHO) is
187 indicated in the figure legends.

188

189 **2.2 POC and PON measurements**

190 Each day, 10 mL of culture was filtered on pre-combusted GF/F filters (5 h, 450 °C)
191 for the POC and PON concentration measurements. The filters were dried overnight in an
192 oven at 50 °C. The POC and PON levels were measured on the same filter using a Carlo Erba
193 NA 2100 CN analyzer coupled to a Finnigan Delta S mass spectrometer (Nieuwenhuize et al.
194 1994). The detection limit was 5 and 1 µg for POC and PON, respectively, with a standard
195 error of 2-3%.

196

197 **2.3 Prokaryotic carbon and nitrogen concentration**

198 The prokaryotic cells were counted over time at each day-point of the degradation
199 experiment to evaluate their growth. Total and free prokaryotes were counted before and after
200 filtration on a 0.3 μ m pore size filter, respectively, in 10 mL samples stained with DAPI (4',6-
201 diamidino-2-phenylindole). The number of attached prokaryotes was calculated by
202 subtracting the number of free-prokaryotes in the 0.3 μ m filtrate from the total prokaryote
203 number. It is important to note that to detach prokaryotes from diatomaceous particles a
204 sequestering/deflocculating agent is added to the total sample (Velji and Albright, 1986).
205 Then the sample was centrifuged at low speed to remove large particles without causing
206 sedimentation of bacteria.

207 The amount of prokaryotic carbon during the degradation experiment was calculated
208 using the conversion factors (20 and 50 x 10⁻¹⁵ molC cell⁻¹ for the free and attached
209 prokaryotes, respectively) proposed by Turley and Mackie (1994). Similarly, the amount of
210 prokaryotic nitrogen was calculated using the N/C ratio of 0.28 proposed by Fagerbakke et al.
211 (1996). Thus, the organic carbon from the diatoms was defined as POC - POC_{attached prokaryotic-C},
212 and the organic nitrogen from the diatoms was defined as PON - PON_{attached prokaryotic-N}.

213

214 **2.4 Particulate carbohydrates (PCHO) analysis**

215 **2.4.1 PCHO extraction and isolation**

216 Similar to the POC and PON measurements, 10 mL of culture was filtered on GF/F
217 filters for the PCHO analysis. The filters were cut with clean scissors and transferred to 15
218 mL glass tubes with Teflon-lined screw caps to which 6 ml of 1.2 M H₂SO₄ was added. The
219 samples were bubbled with N₂ and hydrolyzed in a sand bath for 3 h at 100 °C (Cowie and
220 Hedges, 1984; Panagiotopoulos and Wurl, 2009). The hydrolysis was stopped by placing the
221 tubes in an ice bath for 5–10 min. The samples were neutralized with pre-combusted CaCO₃

222 (450 °C for 5 h) and centrifuged 3–4 times at 4000 rpm for 5 min. The supernatant was
223 filtered through pre-combusted quartz wool (450 °C for 5 h) and pipetted into scintillation
224 vials. The vials were maintained at 4 °C until the time of analysis (this time never exceeded
225 24 h).

226

227 **2.4.2 Liquid chromatography**

228 A Dionex ICS-3000 anion exchange chromatograph fitted with a pulsed amperometric
229 detector (HPAEC-PAD) was used for all PCHO analyses. The separation of the PCHO was
230 performed on a Dionex CarboPac PA-1 analytical column and a Dionex CarboPac PA-1 guard
231 column. An amino trap was placed before the guard column to retain the amino acids and
232 similar compounds, which may interfere with the PCHO analysis. The analytical column, the
233 guard column, and the amino trap were placed into a thermal compartment set at 17 °C
234 (Panagiotopoulos et al., 2012). Sugars were detected by an electrochemical detector (ED40-
235 Dionex) set in the pulsed amperometric mode (standard quadruple potential).

236 Ten individual monosaccharides were detected in the hydrolysates of the particulate
237 organic material, including deoxysugars (fucose, and rhamnose), pentoses (arabinose, ribose,
238 and xylose), one amino sugar (glucosamine), hexoses (galactose, glucose, and mannose), and
239 one acidic sugar (galacturonic acid). The neutral and amino sugars were separated with an
240 isocratic 19 mM NaOH elution at 17 °C (eluent A: 20 mM NaOH; eluent B: Milli Q water).
241 Galacturonic acid was detected in a separate analysis using a gradient of two mobile phases
242 (eluent C: 1 M NaOH; eluent D; 0.5 M CH₃COONa) according to Panagiotopoulos et al.
243 (2012). The flow rate was set at 0.7 ml min⁻¹ for the neutral and acidic sugar analyses. The
244 data acquisition and processing were performed using the Dionex software Chromeleon[®]. The
245 analytic errors calculated by the coefficients of variation of the repeated injections of a

246 standard solution of 50 nM/sugar were 5-10% and 0.9-2.0% (n = 6) for the peak area and the
247 retention time, respectively.

248

249 **2.5 Statistical analysis and kinetic parameters estimation**

250 To compare the contributions of the monosaccharides to the diatom composition in the
251 three treatments at day 1 (triplicates), a *Kruskal-Wallis* test was performed using the R
252 freeware (R Core Team, 2012). Our null hypothesis was that there is no difference in the
253 monosaccharide contributions between the batches. We fixed the significance level at 5%. For
254 each comparison showing a significant difference, a multiple comparison between the
255 treatments was used to determine the batch that was different (Giraudoux, 2012).

256 The degradation rate constants of the bulk parameters (POC and PON) were calculated
257 assuming two pools of organic matter (Moriceau et al., 2009). These two pools can be
258 successively or simultaneously degraded and a 0D model can be applied to estimate the
259 different degradation rate constants.

260 Statistically, the POC and DON data are best fitted with the model using two
261 successive exponential decay equations, as follows:

$$262 \quad C(t) = C_0 \exp(-k_1 t), \quad 0 < t < t_s \quad (1)$$

$$263 \quad C(t) = C(t_s) \exp(-k_2(t-t_s)), \quad t > t_s \quad (2)$$

264 $C(t)$ represents the concentration at day t , C_0 is the initial concentration, t is the time in
265 days, k_1 and k_2 are the two degradation rate constants, and t_s is the substitution time at which
266 the degradation rate constant shifts from k_1 to k_2 .

267 Total carbohydrate (PCHO) and individual monosaccharide concentration values were
268 best fitted into the model using only one exponential decay equation, which is in agreement
269 with previous studies (Giroldo et al., 2003; Goutx et al., 2007; Moriceau et al., 2009),
270 according to the following equation :

271 $C(t) = C_0 \exp(-kt)$ (3)

272 The kinetic parameters for the monosaccharide degradation were calculated with a
273 non-linear least square model using the *nls* function in the R freeware (R Core Team, 2012).
274 Finally, the *t-test* was used to test the null hypothesis on our measured parameters (POC,
275 PON, and PCHO).

276

277 **3. Results**

278 **3.1 Initial observations**

279 At the beginning of the biodegradation experiment, diatom cell concentrations were
280 1.80×10^8 cell L⁻¹ in the ‘Nutrient-replete’ batch, 2.11×10^8 cell L⁻¹ in the ‘Si-stress’ batch,
281 and 3.02×10^8 cells L⁻¹ in the ‘N-stress’ batch (Table 1). The N- and Si-stress growth
282 conditions induced an increase in the carbon content per cell compared with the ‘Nutrient-
283 replete’ diatoms (8.14, 14.39, and 17.41 pmol cell⁻¹ in the ‘Nutrient-replete’, ‘N-stress’, and
284 ‘Si-stress’ batches, respectively) (Table 1).

285 The ‘Si-stress’ and ‘N-stress’ diatoms had a lower cellular volume than the ‘Nutrient-
286 replete’ diatoms. The ‘N-stress’ and the ‘Si-stress’ cells contained approximately two times
287 the amount of organic carbon than the ‘Nutrient-replete’ cells (Table 1), which was even more
288 pronounced when estimated on a per volume liter basis (12.47, 12.76, and 5.47 pmol cell⁻¹,
289 respectively). The organic nitrogen content did not follow the organic carbon patterns and was
290 lower in the ‘N-stress’ cells (0.73 pmol cell⁻¹) than in the ‘Nutrient-replete’ (1.17 pmol cell⁻¹)
291 and ‘Si-stress’ cells (1.51 pmol cell⁻¹) (Table 1). Similar to previous results, these differences
292 were observed when estimated on a per volume basis.

293 The concentration of the prokaryotic inoculums was of the same order of magnitude in
294 all of the batches at T₀ indicating the same bacterial number ($\sim 10^9$ cell L⁻¹) at the beginning
295 of the experiments (Table 1). The prokaryotic concentrations in the three batches showed the

296 same global trend over time, reaching a maximum at day 3 followed by a decrease until
297 reached a steady state (Fig. 2). It is worth noting that prokaryotic concentrations reached this
298 steady state ($\sim 40 \times 10^9$ cell L⁻¹) in the ‘Nutrient-replete’ batch much earlier (at day 6) than in
299 the ‘N-stress’ and ‘Si-stress’ batches (after ~ 15 days) (Fig. 2). This difference may be
300 explained by the initially higher concentrations of the POC in the N- and Si- stressed cell
301 batches (Table 1).

302 Our results showed an increase in the POC concentrations (approximately 7-30% of
303 the initial POC) which was observed between T₀ and T₁ in all three batches (Fig. 2). Then
304 POC concentrations decreased over time till the end of the experiment. The growth of the
305 attached prokaryotes at day 1 (Fig. 2) explained only 7.5%, 0.9% and 1.2% of the increase of
306 the POC at day 1 in the ‘Nutrient-replete’, ‘N-stress’, and ‘Si-stress’ experiments,
307 respectively. This result further indicates that the increase in POC at day 1 is most likely
308 related to a combination of biotic and abiotic processes at the beginning of the degradation
309 experiments (e.g. agglomeration of POC due to heterogeneity, prokaryotes growth, a low TEP
310 production by bacteria) including analytical error (Fig. 3). The increase in the POC at day 1
311 may also be related to the absorption/desorption phenomena of the suspended particles on the
312 bottle wall during biodegradation. These observations (increase of POC at day 1) have been
313 previously reported in particle or diatom biodegradation experiments (Panagiotopoulos et al.,
314 2002; Engel et al., 2009).

315 After day 1, POC decreased over time while we observed an increase in the bacterial
316 numbers, which typically reflects the decomposition pattern of TW-POC. For all of these
317 reasons mentioned above, we have chosen to consider the data at T₁ as the beginning of the
318 degradation.

319 Similar to the POC levels, the PON concentrations also showed an increase at day 1 in
320 all of the batches (+ 70.1, + 58.4 and + 55.6% of the initial PON concentrations in the

321 'Nutrient-replete', 'N-stress' and 'Si-stress' batches, respectively). Using conversion factors
322 to estimate the organic nitrogen contribution from the prokaryotes (see the Materials and
323 Methods section), the prokaryotic nitrogen accounted for 13, 10 and 8% of the total PON at
324 day 1 in the 'Nutrient-replete', 'N-stress' and 'Si-stress' batches, respectively.

325 The C/N ratio was equal to 7.0 at the beginning of the degradation experiment in the
326 'Nutrient-replete' batch, which is in the range of the previously reported values for TW (C/N
327 = 5-9; Brzezinski, 1985; De La Rocha et al., 2010). This ratio was strongly influenced by the
328 nutrient stress, with an increase of up to 11.5 in the 'Si-stress' cells and 19.7 in the 'N-stress'
329 cells.

330

331 **3.2 Initial particulate carbohydrate composition (PCHO)**

332 Similar to the POC, the initial concentrations of the PCHO-C in the 'N-stress' and 'Si-
333 stress' cells on a per volume basis were approximately two and four times higher than those in
334 the 'Nutrient-replete' cells (0.22, 0.40, and 0.11 pmol cell⁻¹, respectively). Note that the
335 PCHO analyses do not discriminate between the PCHO arising from diatoms and those from
336 prokaryotes.

337 Similar to the POC levels, the PCHO-C concentrations also peaked at day 1 and
338 increased by 3.7%, 2.4%, and 1.1% of their initial concentrations in the 'Nutrient-replete', 'N-
339 stress' and 'Si-stress' batches, respectively. Therefore, as observed with the POC degradation,
340 the PCHO-C degradation rate constants were calculated from day 1. The monosaccharide
341 composition at day 1 was dominated by ribose, galactose, and glucose in all of the batches,
342 which accounted for more than 60 mol% of the total PCHO pool (Table 2).

343 The 'Nutrient-replete' batch was characterized by a higher ribose contribution (22
344 mol%) compared with the 'N-stress' and 'Si-stress' batches (4 and 11 mol%, respectively) at
345 day 0, whereas the contribution of galactose varied only slightly between the three batches (29

346 to 38 mol%; Table 2). The contribution of glucose was significantly higher in the ‘N-stress’
347 batch compared with the ‘Nutrient-replete’ batch (Kruskal-Wallis test, $n = 9$, $p < 0.05$). The
348 ribose concentrations and yields (Rib.-C/PCHO-C %) rapidly decreased over time in all of the
349 experiments, indicating a selective extraction of this monosaccharide from the PCHO pool
350 (Table 2). Interestingly, the ‘Nutrient-replete’ batch was particularly enriched in galacturonic
351 acid (~8 mol%) compared with the ‘N-stress’, and ‘Si-stress’ batches (< 2 mol%; Table 2).
352 Finally, none of the other monosaccharides showed significant initial differences (at day 1)
353 among the ‘Nutrient-replete’, ‘N-stress’, and ‘Si-stress’ batches.

354

355 **3.3 Organic matter degradation**

356 **3.3.1 Bulk parameters (POC and PON)**

357 As indicated above, an increase in the POC concentrations (approximately 7-30% of
358 the initial POC) was observed at day 1 in the three batches. Therefore, the biotic degradation
359 kinetics were calculated beginning at day 1. The POC degradation followed similar patterns in
360 the three batches, with a first period of degradation in which the POC degraded faster
361 followed by a second period of degradation in which the POC was degraded more slowly
362 (Fig. 3a). The degradation rate constants of the first period were similar in the three batches
363 ($0.11 \pm 0.03 \text{ d}^{-1}$, $0.096 \pm 0.002 \text{ d}^{-1}$, and $0.11 \pm 0.01 \text{ d}^{-1}$; Table 3); however, this was not the
364 case for the substitution time, which was different among the three batches ($t_s = 5.9 \pm 0.6 \text{ d}$,
365 $11.1 \pm 0.2 \text{ d}$ and $8.5 \pm 0.2 \text{ d}$).

366 At the end of the rapid degradation period, ~40% of the POC from the ‘Nutrient-
367 replete’ diatoms was degraded, whereas this amount was ~60% for the N- and Si- stressed
368 TW during the same period. During the second period, the POC was degraded at a
369 significantly slower rate, with degradation rate constants of $0.040 \pm 0.001 \text{ d}^{-1}$, 0.018 ± 0.001
370 d^{-1} , and $0.014 \pm 0.001 \text{ d}^{-1}$ for the ‘Nutrient-replete’, ‘N-stress’, and ‘Si-stress’ batches,

371 respectively. Interestingly, the POC concentrations reached a “plateau” after 25 days of
372 degradation and accounted for 27% of the initial POC in all three of the batches (Fig. 3a).

373 The degradation rate constants of the PON were consistently higher in the ‘Nutrient-
374 replete’ batch for both of the pools (k_1 and k_2) than in the ‘N- and Si-stress’ batches (Table 3;
375 Fig. 3b). The degradation rate constants of the PON measured in the ‘N- and Si-stress’
376 batches only differed for the k_1 constant rates (Table 3). The second pool of the PON
377 degraded with a similar degradation rate constant in the ‘N- and Si-stress’ batches ($k_2 \approx 0.020$
378 ± 0.001 d⁻¹). The t_s value was one half the value in the ‘Nutrient-replete’ batch (5.0 ± 0.6 d)
379 compared with the ‘N- and Si-stress’ batches ($\sim 10.0 \pm 0.6$ d). Therefore, at the end of the
380 biodegradation experiment (30 days), only 18% of the initial PON remained in the ‘Nutrient-
381 replete’ batch, whereas 40% and 55% remained in the ‘Si-stress’ and the ‘N-stress’ batches,
382 respectively.

383

384 3.3.2 Particulate carbohydrates (PCHO)

385 The degradation rate constants for the total PCHO-C were slightly lower but not
386 significantly different in the ‘N-stress’ and ‘Si-stress’ batches (0.04 ± 0.01 d⁻¹) than in the
387 ‘Nutrient-replete’ batch (0.05 ± 0.01 d⁻¹; Table 3; Fig. 4). At the end of the 30 days of
388 degradation, 26% of the total PCHO-C remained in the ‘Nutrient-replete’ batch, whereas
389 PCHO-C represented $\sim 35\%$ in the ‘N-stress’ and ‘Si-stress’ batches.

390 The degradation rate constants of the individual monosaccharides showed important
391 differences in their decay (Table 3). Ribose was the monosaccharide with the highest
392 degradation rate constants ($k = 0.073$ - 0.215 d⁻¹) followed by glucose ($k = 0.028$ - 0.071 d⁻¹),
393 and galactose ($k = 0.018$ - 0.060 d⁻¹). A slight, non-significant decrease in the galactose
394 concentrations was observed in the ‘N-stress’ batch, with a degradation rate constant three
395 times lower than that of the ‘Nutrient-replete’ and ‘Si-stress’ batches ($k = 0.02 \pm 0.01$ d⁻¹

396 versus $0.05 \pm 0.01 \text{ d}^{-1}$ and $0.06 \pm 0.02 \text{ d}^{-1}$, respectively, Fig. 5a). Similarly, the ribose
397 degradation rate constants in the ‘Nutrient-replete’ and ‘N-stress’ batches were very different
398 and three-times lower in the latter ($k = 0.21 \pm 0.05 \text{ d}^{-1}$ and $0.073 \pm 0.007 \text{ d}^{-1}$ in the ‘Nutrient-
399 replete’ and ‘N-stress’ batches, respectively, Fig. 5b). The high variability of the ribose
400 concentrations in the ‘Si-stress’ batch did not allow an accurate estimation of the kinetic
401 parameters ($k = 0.07 \pm 0.04$, $p > 0.1$). This result was also the case for glucose, which showed
402 a non-significant degradation rate constant very close to that measured in the ‘Nutrient-
403 replete’ batch (Table 3; Fig. 5c). In the ‘N-stress’ batch, the glucose degradation rate constant
404 was two times higher than that of the ‘Nutrient-replete’ batch ($k = 0.07 \pm 0.04 \text{ d}^{-1}$) indicating
405 the presence of a labile pool of glucose-containing molecules.

406 The degradation rate constants of the other monosaccharides were variable, ranging
407 from <0 (arabinose) to 0.027 d^{-1} (rhamnose). As a general trend, the degradation rate
408 constants of these individual monosaccharides were higher in the ‘Nutrient-replete’ batch
409 compared with the ‘N and Si- stress’ batches.

410 **4. Discussion**

411 **4.1 Effect of N- and Si-starvation on the initial *Thalassiosira weissflogii* composition**

412 The effect of nutrient stress, including starvations, on the biochemical content (sugars,
413 amino acids, and lipids) of diatoms has been addressed in previous studies for several diatom
414 species (De La Rocha et al., 2010; Hou et al., 2007; Liu et al., 2012). These studies have
415 shown dissimilarities in the physiological responses of the diatom, indicating a specific
416 response against nutrient stress (Palmucci et al., 2011; Richardson and Cullen, 1995; Shifrin
417 and Chisholm, 1981; Waite et al., 1992) and are in agreement with the present study. Our
418 results showed that nitrogen and silicon starvations induced an increase in the carbon content
419 per cell in TW (Table 1). Other studies have reported a decrease in the N content per cell

420 during N starvation, whereas no changes have been observed during Si starvation (De la
421 Rocha et al. 2010). Our results showed that the N content per cell also decreased during N-
422 starvation and slightly increased during Si- starvation (Table 1) indicating that N- and/or Si-
423 starvations have different effects on the carbon and nitrogen content of TW.

424 The carbohydrate (PCHO) concentrations in the 'Nutrient-replete' cells were 2-3 times
425 lower than those found in the 'N-stress' and 'Si-stress' cells (Table 2), suggesting an increase
426 in the PCHO levels during starvations, which is in agreement with previous investigations
427 performed in other diatoms species (*T. pseudonana*; Harrison et al., 1990). Other studies
428 performed on TW employing similar nutrient starvation conditions have reported a decrease
429 in the amino acid and lipid content (Klein Breteler et al., 2005; Martin-Jézéquel, 1992; Shifrin
430 and Chisholm, 1981). These results suggest that nutrient starvation has different effects on the
431 organic matter components of the diatoms (carbohydrates, lipids, and amino acids).
432 Carbohydrates in diatoms are generally divided into cellular and extracellular polysaccharides
433 (Myklestad, 1995). In diatoms, it is well known that the genus *Thalassiosira* releases low
434 levels of extracellular polysaccharides, primarily composed of glucose (Urbani et al., 2005),
435 compared with another genus, such as *Chaetoceros* (Myklestad, 1995). The amount of
436 extracellular polysaccharides released under a nutrient stress accounts for approximately 3%
437 of the total cellular carbohydrate in TW (Myklestad, 1995). Carbohydrates are molecules that
438 are primarily composed of carbon atoms, and their release as extracellular polysaccharides
439 (EPS) during stress conditions may decrease the C/N ratio of the diatom cells to their 'initial'
440 value (C/N value of = 5-7).

441 The changes in the carbohydrate concentration during stress conditions were also
442 reflected in their individual sugar monomers, which have never been thoroughly examined in
443 previous studies (Table 2). The relative abundance of most of the monosaccharides increased
444 during Si-starvation (except for ribose and galacturonic acid), whereas the primary differences

445 for the N-starvation experiment were observed in the relative abundances of glucose, ribose,
446 and xylose. N-starvation strongly affected the glucose content of the cells (Table 2).
447 Therefore, the high increase in the glucose relative abundance may suggest a preferential
448 synthesis of glucose-rich polymers such as laminarin which are well known to be storage
449 molecules in diatoms (Størseth et al., 2005). The high relative abundance of ribose in the
450 'Nutrient-replete' cells most likely reflects the better physiological status of these cells
451 because ribose-containing molecules (e.g., ATP and RNA) are involved in energy
452 metabolism. Other studies have shown a decrease in the RNA synthesis in the 'N-stress'
453 diatoms, implying a decrease in the ribose content of the cells, which is in agreement with our
454 results (Hockin et al., 2012; Mock et al., 2008). High amounts of ribose in marine particulate
455 organic matter is generally attributed to fresh material (Panagiotopoulos and Sempéré, 2005a,
456 2007), but it can also imply a good physiological status of the 'diatom' cells in the
457 investigated sampling area.

458 The above results clearly suggest that Si-starvation may have a more pronounced
459 effect on the cell's physiological status than on its metabolism functions. This result may
460 indicate that silica-stress cells have lower energy requirements (no synthesis of glucose
461 polymers) than nitrogen-stress cells. This result is in agreement with previous results on *T.*
462 *pseudonana*, suggesting an uncoupling of Si with C metabolism (Claquin et al., 2002).

463

464 **4.2 Effect of N- and Si- starvation on *Thalassiosira weissflogii* organic matter** 465 **degradation**

466 As indicated above, the kinetic calculations of the POC and PON degradation
467 suggested the presence of two pools of organic matter with different degradation rate
468 constants (Table 3). These results suggest that both of these pools are composed of relatively
469 biodegradable molecules, and certain of these molecules are most likely produced during

470 starvation (extracellular sugars; Table 3 and Fig. 3a). Our results also showed that although
471 the first order degradation rate constants (k_1) of the ‘nutrient-replete’, ‘N-stress’, and ‘Si-
472 stress’ for the TW-POC were nearly similar during degradation, they corresponded to
473 different substitution t_s values. The higher t_s values were observed during the nutrient stressed
474 TW- POC degradation (t_s values of 8.5-11.4 days) compared with the “Nutrient replete” cells
475 (t_s value of 5.9 days; Table 3). These results clearly indicate that the TW-intracellular
476 molecules that constitute the labile TW-POC (first order rate constants) are degraded over a
477 longer period in which the TW cells are submitted to “stress” conditions. This result may be
478 partially explained by the increase in the carbon content of the TW cells in which labile
479 compounds, such as carbohydrates, are produced during stress-conditions; therefore,
480 additional time for their degradation is required (Table 2). The degradation rate constants of
481 the second pool (k_2) during the TW-POC degradation were nearly similar for the “stress-cells”
482 but significantly lower than those of the ‘Nutrient-replete’ cells ($k_{Si-stress} \sim k_{N-stress} \ll k_{nut.-rep.}$;
483 Table 3). These results indicate that the stress-conditions may increase the residence time (k^{-1})
484 of less labile organic molecules, which may affect their bioavailability in the environment.

485 In contrast to the POC, the first order degradation rate constants (k_1) of PON were
486 clearly different between each batch (Table 3, Fig. 3b). Our results indicated that TW-PON
487 appeared to become less labile after the N- and Si- starvations. These differences were
488 reflected in the amount of diatom PON remaining at the end of each experiment (17.4%,
489 34.7% and 51.1% of the initial diatom PON in the ‘Nutrient-replete’, ‘Si-stress’, and ‘N-
490 stress’ batches, respectively). These results may suggest a N-utilization from the TW
491 intracellular N-compounds (proteins, nucleic acids, and/or ATP), which are well known to be
492 very labile (Hockin et al., 2012). This result concurs with the low initial concentrations of
493 ribose recorded in the “N- and Si-stress” TW-cells (Table 3), indicating that the ATP

494 molecules (ribose and N-nucleobases-rich) are most likely the first to be exhausted at the
495 beginning of the N-starvation.

496 Although the POC/PON ratios were high at the beginning of the degradation for the
497 ‘N- and Si-stress’ cells, they reached values close to the Redfield C/N ratio after ~ 5-11 days
498 of degradation (Fig. 6; Sarthou et al., 2005). This result suggests a preferential prokaryotic
499 degradation of excess C- containing compounds and may explain the high degradation rate
500 constant of glucose (an N-free compound) obtained in the ‘N-stress’-experiment (most likely
501 storage compounds) (Table 3; Fig. 5c). Interestingly, similar C/N ratios (6.1-6.7) have been
502 obtained for sediment trap material collected from the Pacific Ocean (Hernes et al. 1996). The
503 authors have interpreted these low values as a non-selective degradation of OC versus ON.
504 Alternatively, this result may be due to a preferential selectivity that coincidentally maintains
505 the low C/N values. Our results agree with these features, indicating a non-coincident
506 selective degradation of excess C- and N-containing molecules.

507 The degradation rate constants of the PCHO were consistently lower than the first
508 order degradation rate constants of the POC ($k_1 = 0.096-0.11 \text{ d}^{-1}$; Table 3) but higher than the
509 second order degradation rate constants of the POC ($k_2 = 0.018-0.040 \text{ d}^{-1}$), indicating that
510 carbohydrates are most likely the second most labile component in TW after amino acids. The
511 PCHO degradation rate constants were higher than the individual monosaccharides, except for
512 ribose, which exhibited the highest rates in all of the experiments (Table 3). Therefore, it
513 appears that the PCHO rate constants reflect an average of the different degradation rates
514 corresponding to each monosaccharide, indicating differences in their initial macromolecular
515 origin (e.g. storage vs structural carbohydrates).

516 For example, the galactose degradation rate constants were higher in the ‘Nutrient-
517 replete’ and ‘Si-stress’ cell degradation experiments than in the ‘N-stress’ experiment (Table
518 3; Fig. 5a). This monosaccharide is primarily found in cell wall polysaccharides (Cowie and

519 Hedges, 1996; Hecky et al., 1973), whereas it is also reported in excreted exopolymeric
520 substances (Giroldo et al., 2003). Based on the ectoenzymatic bacterial activities in sediments,
521 Arnosti (2000) has suggested that the former could be less labile than the latter. Based on the
522 above literature observations and the higher degradation rate constants observed for the
523 ‘Nutrient-replete’ and ‘Si-stress’ experiments (Table 3), we may hypothesize that galactose
524 would primarily originate from the excretion of the EPS (in the case of the ‘Nutrient-replete’
525 and ‘Si-stress’ experiments), which are known to be stimulated during nutrient deficiency.
526 Alternatively, galactose may also originate from the cell wall polysaccharides in the ‘N-stress’
527 cell experiment based on its low degradation constant.

528 The ribose degradation rate constants showed important differences among the
529 starvation experiments. The high degradation rate constant recorded for the ‘Nutrient-replete’
530 experiment reflects the good physiological status of the TW cells and agrees with the elevated
531 ribose concentrations measured at T_0 (Table 3, Fig. 5b). This high rate most likely illustrates
532 the hydrolysis of ATP polymers (rich in ribose), whereas the low rates measured in N- and Si-
533 stress cells most likely indicate the exhaustion of the ATP molecules at the beginning of the
534 N-starvation (see above). This result is further supported by the similarity of the first order
535 decay constants of the PON and those of ribose for all of the biodegradation experiments
536 (Table 3).

537 Similarly, the degradation rate constants measured for glucose may provide
538 indications about the nature of the original polymer. Glucose may originate from laminarin
539 (Størseth et al., 2005) or callose (Tesson and Hildebrand, 2013), which are sugar-polymers
540 involved in energy storage (laminarin) or fibrillar structure (callose). The high degradation rate
541 constant (indicating increased bioavailability) obtained for the glucose in the ‘N-stress’ TW
542 most likely suggests that glucose may originate from laminarin (Table 3; Fig. 5c).

543 Our results also showed that the concentrations of some of the monosaccharides
544 showed a small increase after day 1. This was especially the case for arabinose, galacturonic
545 acid, and mannose (Table 2). This result may be related to the increase of the prokaryotic
546 concentration which peaked at day 3 (Fig. 2), most likely suggesting that these
547 monosaccharides may be *de novo* produced by prokaryotes. However, the prokaryotic carbon
548 represented a small percentage of this increase (see above) and cannot solely explain the
549 increase in the concentrations of these sugars.

550 The increase in the mannose and arabinose concentrations in ‘Si-stress’ batch may be
551 related to other factors, such as a release of polysaccharides from the frustule of TW, which is
552 dissolved slowly over time. Earlier studies on four different diatom species indicated that the
553 polysaccharides released after the dissolution of the frustules are primarily composed of a
554 mannose backbone bearing uronic acid residues (Chiovitti et al., 2005). In our study, the
555 degradation rate constant of galacturonic acid in the ‘Si-stress’ batch was completely different
556 from that of the two other batches (Table 3). This result may be explained by a modified
557 frustule structure affected by the Si starvation (Moriceau et al., 2007; Soler, 2010). This
558 finding strongly agrees with the high correlation between the mannose and galacturonic acid
559 concentrations over time in the ‘Nutrient-replete’ batch ($r = 0.88$).

560

561 **4.3 Biogeochemical implications on the vertical transport of the nutrient-stressed TW cells**

562 In a marine environment, diatoms are often subjected to nutrient depletion depending
563 on the environmental conditions. Although it has been suggested that diatoms may regulate
564 their buoyancy to sink into a deeper nutrient-rich layer of the euphotic zone, the effect of the
565 nutrient stress on their morphology is not well known (Kemp et al., 2006 and references
566 therein). The *Thalassiosira* species, in particular, have been suggested to be very nutrient-
567 sensitive, which significantly affects their sinking rate (Waite et al., 1992). Other studies have

568 demonstrated that nutrient-stressed TW cells increase their carbohydrate content, resulting in
569 an increase in their density and their aggregation; therefore, they sink rapidly in the water
570 column (Richardson and Cullen, 1995). Our results also showed an increase in the
571 carbohydrate content of the TW cells under N- and Si-depleted conditions, which may
572 potentially impact the behavior of TW cells (changes in sinking rates, aggregation etc) in the
573 natural environment. Furthermore, the degradation rate constants (k_1 , and k_2) of the nutrient
574 limited cells generally decreased compared with the nutrient-replete cells (Table 3), which
575 further may imply a potentially higher amount of carbon for export under nutrient-stress
576 conditions.

577 On the other hand, other studies indicated that the decrease in the cell size due to the
578 nutrient-limitation may attenuate the sinking rates because of the dissolution of silicon, which
579 forms the cell frustule, resulting in lighter TW cells (De la Rocha and Passow, 2007; Boutorh,
580 2014). Our experiments also showed a decrease in the bSiO₂ content in the stressed TW cells
581 (Table 1). Overall, these results highlight the complexity of evaluating the relationship
582 between the environmental factors (nutrient-limitation) and the sinking velocity of diatom
583 frustules. These factors clearly influence the sequestration of organic carbon in the deep ocean
584 at the spatial (differences in species composition) and temporal (differences in physiological
585 status) scales and clearly have an important effect on the microbial carbon pump.

586

587 **Summary and concluding remarks**

588 This study explored the degradation features of the TW cells grown under nutrient-
589 stress conditions (N- and Si- limitations), similar to those occurring in a natural environment.
590 Our results showed that the TW stressed-cells increased their carbon content (approximately
591 two times) and their C/N ratios (2-3 times) compared with the ‘Nutrient-replete’ cells (Table
592 1; Fig. 6). This carbon increase was accompanied by a decrease in the bSiO₂ in the nutrient-

593 stressed cells, indicating a structural modification of the TW frustule. From a chemical
594 composition view point, this increase in the carbon was essentially reflected in the
595 carbohydrate component of the TW cells. Hence, the carbohydrate (PCHO) concentrations in
596 the 'Nutrient-replete' cells were 2-3 times lower than those found in the 'N-stress' and 'Si-
597 stress' cells (Table 2) suggesting an increase in the PCHO content during starvation. The 'N-
598 stress' and 'Si-stress' cells were characterized by higher amounts of glucose (5-32 mol%) and
599 xylose (13-19 mol%) compared with the 'Nutrient-replete' cells, which were dominated by
600 ribose (22 mol%), indicating differences in the physiological status of the TW cells and/or
601 the synthesis of storage/structural polysaccharides under different nutrient growth conditions.

602 The biodegradation experiments of the 'Nutrient-replete', 'N-stress', and 'Si-stress'
603 TW cells showed that the first order degradation rate constants for the POC were similar ($k_1 =$
604 $0.096-0.113 \text{ d}^{-1}$) but were characterized by different substitution times, indicating that
605 intracellular and labile TW compounds require longer times to be degraded under stress
606 conditions (Table 3). The second order degradation rate constants (k_2) of the POC were
607 approximately two times higher for the 'Nutrient-replete' cells than the 'N-stress' and 'Si-
608 stress' cells, indicating that nutrient limited conditions may increase the residence time (k^{-1}) of
609 less labile intracellular TW compounds. The PCHO degradation rates were between the first
610 and the second order degradation rates of the POC, suggesting that the carbohydrates are
611 most likely the second most labile component of TW after the amino acids.

612 Ribose, glucose, and galactose exhibited the highest degradation rate constants in the
613 various experiments which further reflects the differences in their initial macromolecular
614 origin due to different C and N allocation (e.g. storage vs structural carbohydrates) under
615 nutrient-limited conditions and highlights the changes in the organic matter quality during
616 degradation.

617

618 *Acknowledgments*

619 We thank D. Delmas for the prokaryote counting during the degradation experiment and
620 C. Labry for the seawater sampling at the Brest Somlit station. We also thank A. Masson for
621 the POC/PON measurements as well as the two anonymous reviewers for their constructive
622 comments. This study was supported by the UTIL (LEFE/CYBER, CNRS/INSU) and
623 MANDARINE (Région Provence Alpes Côte d'Azur) projects. M. Suroy was supported by a
624 Ph.D grant from Aix-Marseille University.

625

626

627

628

629

630

631

632

633

634

635

636

637

638 *References*

- 639 Arnosti, C., 2000. Substrate specificity in polysaccharide hydrolysis: contrasts between
640 bottom water and sediments. *Limnol. Oceanogr.* 45, 1112–1119.
- 641 Aumont, O., Maier-Reimer, E., Blain, S., Monfray, P., 2003. An ecosystem model of the
642 global ocean including Fe, Si, P colimitations. *Global Biogeochem. Cy.* 17, 1–26.
- 643 Bidle, K.D., Manganello, M., Azam, F., 2002. Regulation of oceanic silicon and carbon
644 preservation by temperature control on bacteria. *Science* 298, 1980–1984.
- 645 Boutorh, J., 2014. Impact des conditions nutritionnelles sur la dissolution de la silice
646 biogénique des diatomées à travers l'étude de la variabilité de la structure biphasique du
647 frustule. Ph.D. Thesis, Université de Bretagne occidentale, France, pp 181.
- 648 Brown, M.R., Jeffrey, S.W., Volkman, J.K., Dunstan, G.A., 1997. Nutritional properties of
649 microalgae for mariculture. *Aquaculture* 151, 315–331.
- 650 Brzezinski, M.A., 1985. The Si:C:N ratio of marine diatoms : interspecific variability and the
651 effect of some environmental variables. *J. Phycol.* 21, 347–357.
- 652 Buesseler, K.O., 1998. The decoupling of production and particulate export in the surface
653 ocean. *Global Biogeochem. Cy.* 12, 297–310.
- 654 Chiovitti, A., Harper, R.E., Willis, A., Bacic, A., Mulvaney, P., Wetherbee, R., 2005.
655 Variations in the substituted 3-linked mannans closely associated with the silicified walls
656 of diatoms. *J. Phycol.* 41, 1154–1161.

657 Chiovitti, A., Higgins, M.J., Harper, R.E., Wetherbee, R., 2003. The complex polysaccharides
658 of the raphid diatom *Pinnularia viridis* (Bacillariophyceae). *J. Phycol.* 39, 543–554.

659 Claquin, P., Martin-Jézéquel, V., Kromkamp, J.C., Veldhuis, M., Kraay, G., 2002.
660 Uncoupling of silicon compared with carbon and nitrogen metabolisms and the role of
661 the cell cycle in continuous cultures of *Thalassiosira pseudonana* (Bacillariophyceae)
662 under light, nitrogen, and phosphorus control. *J. Phycol.* 38, 922–930.

663 Cowie, G.L., Hedges, J.I., 1984. Carbohydrate sources in a coastal marine environment.
664 *Geochim. Cosmochim. Acta* 48, 2075–2087.

665 Cowie, G.L., Hedges, J.I., 1996. Digestion and alteration of the biochemical constituents of a
666 diatom (*Thalassiosira weissflogii*) ingested by an herbivorous zooplankton (*Calanus*
667 *pacificus*). *Limnol. Oceanogr.* 41, 581-594.

668 De La Rocha, C.L., Passow, U., 2007. Factors influencing the sinking of POC and the
669 efficiency of the biological carbon pump. *Deep-Sea Res. PT II* 54, 639–658.

670 De La Rocha, C.L., Terbrüggen, A., Völker, C., Hohn, S., 2010. Response to and recovery
671 from nitrogen and silicon starvation in *Thalassiosira weissflogii*: growth rates, nutrient
672 uptake and C, Si and N content per cell. *Mar. Ecol. Prog. Ser.* 412, 57–68.

673 Duhamel, S., Moutin, T., Van Wambeke, F., Van Mooy, B., Raimbault, P., Chaustre, H.,
674 2007. Growth and specific P-uptake rates of bacterial and phytoplanktonic communities
675 in the Southeast Pacific (BIOSOPE cruise). *Biogeosciences* 4, 941-956.

676 Engel, A., Abramson, L., Szlosek, J., Liu, Z., Stewart, G., Hirschberg, D., Lee, C., 2009.
677 Investigating the effect of ballasting by CaCO₃ in *Emiliania huxleyi*, II: Decomposition
678 of particulate organic matter. *Deep-Sea Res. PT II* 56, 1408–1419.

679 Fagerbakke, K.M., Heldal, M., Norland, S., 1996. Content of carbon, nitrogen, oxygen, sulfur
680 and phosphorus in native aquatic and cultured bacteria. *Aquat. Microb. Ecol.* 10, 15–27.

681 Falkowski, P.G., 1997. Evolution of the nitrogen cycle and its influence on the biological
682 sequestration of CO₂ in the ocean. *Nature* 246, 170–170.

683 Giraudoux, P., 2012. pgirmess: Data analysis in ecology. R package version 1.5.4.
684 <http://CRAN.R-project.org/package=pgirmess>.

685 Girollo, D., Vieira, A.A.H., Paulsen, B.S., 2003. Relative increase of deoxy sugars during
686 microbial degradation of an extracellular polysaccharide released by a tropical
687 freshwater *Thalassiosira* sp. (Bacillariophyceae). *J. Phycol.* 39, 1109–1115.

688 Goutx, M., Wakeham, S.G., Lee, C., Duflos, M., Guigue, C., Liu, Z., Moriceau, B., Sempéré,
689 R., Tedetti, M., Xue, J., 2007. Composition and degradation of marine particles with
690 different settling velocities in the northwestern Mediterranean Sea. *Limnol. Oceanogr.*
691 52, 1645–1664.

692 Harrison, P.J., Thompson, P.A., Calderwood, G.S., 1990. Effects of nutrient and light
693 limitation on the biochemical composition of phytoplankton. *J. Appl. Phycol.* 2, 45–56.

694 Harvey, H.R., Tuttle, J.H., Tyler Bell, J., 1995. Kinetics of phytoplankton decay during
695 simulated sedimentation: Changes in biochemical composition and microbial activity
696 under oxic and anoxic conditions. *Geochim. Cosmochim. Acta* 59, 3367–3377.

697 Harvey, H.R., Macko, S.A., 1997. Kinetics of phytoplankton decay during simulated
698 sedimentation: changes in lipids under oxic and anoxic conditions. *Org. Geochem.* 27,
699 129–140.

700 Hecky, R.E., Mopper, K., Kilham, P., Degens, E.T., 1973. The amino acid and sugar
701 composition of diatom cell-walls. *Mar. Biol.* 19, 323–331.

702 Hernes, P.J., Hedges, J.I., Peterson, M.L., Wakeham, S.G., Lee, C., 1996. Neutral
703 carbohydrate geochemistry of particulate material in the central equatorial Pacific. *Deep-*
704 *Sea Res. PT II* 43, 1181–1204.

705 Hildebrand, M., 2002. Lack of coupling between silicon and other elemental metabolisms in
706 diatoms. *J. Phycol.* 38, 841–843.

707 Hockin, N.L., Mock, T., Mulholland, F., Kopriva, S., Malin, G., 2012. The response of
708 diatom central carbon metabolism to nitrogen starvation is different from that of green
709 algae and higher plants. *Plant Physiol.* 158, 299–312.

710 Honda, M.C., Watanabe, S., 2010. Importance of biogenic opal as ballast of particulate
711 organic carbon (POC) transport and existence of mineral ballast-associated and residual
712 POC in the Western Pacific Subarctic Gyre. *Geophys. Res. Lett.* 37, L02605,
713 doi:10.1029/2009GL041521.

714 Hou, J.J., Huang, B.Q., Cao, Z.R., 2007. Effects of nutrient limitation on pigments in
715 *Thalassiosira weissflogii* and *Prorocentrum donghaiense*. *J. Integr. Plant Biol.* 49, 686–
716 697.

717 Iversen, M.H., Ploug, H., 2013. Temperature effects on carbon-specific respiration rate and
718 sinking velocity of diatom aggregates–potential implications for deep ocean export
719 processes. *Biogeosciences* 10, 4073–4085.

720 Kemp, A.E.S., Pearce, R.B., Grigorov, I., Rance, J., Lange, C.B., Quilty, P., Salter, I., 2006.
721 Production of giant marine diatoms and their export at oceanic frontal zones:

722 Implications for Si and C flux from stratified oceans. *Global Biogeochem. Cy.* 20,
723 GB4S04, doi:[10.1029/2006GB002698](https://doi.org/10.1029/2006GB002698).

724 Klein Breteler, W.C.M., Schogt, N., Rampen, S.W., 2005. Effect of diatom nutrient limitation
725 on copepod development: the role of essential lipids. *Mar. Ecol. Prog. Ser.* 291, 125–
726 133.

727 Lahanan, F., Jusoh, A., Ali, N., Lam, A.S., Endut, A., 2013. Effect of conway medium on the
728 growth of six genera of South China Sea marine microalgae. *Bioresource Technol.* 141:
729 75-82.

730 Legendre, L., Rivkin, R.B., 2002. Fluxes of carbon in the upper ocean: regulation by food-
731 web control nodes. *Mar. Ecol. Prog. Ser.* 242, 95–109.

732 Liu, W., Huang, Z., Li, P., Xia, J., Chen, B., 2012. Formation of triacylglycerol in *Nitzschia*
733 *closterium* f. *minutissima* under nitrogen limitation and possible physiological and
734 biochemical mechanisms. *J. Exp. Mar. Biol. Ecol.* 418-419, 24–29.

735 Logan, B.E., Passow, U., Alldredge, A.L., Grossart, H.-P., Simon, M., 1995. Rapid formation
736 and sedimentation of large aggregates is predictable from coagulation rates (half-lives) of
737 transparent exopolymer particles (TEP). *Deep-Sea Res. PT II* 42, 203–214.

738 Lynn, S.G., Kilham, S.S., Kreeger, D.A., Interlandi, S.J., 2000. Effect of nutrient availability
739 on the biochemical and elemental stoichiometry in the freshwater diatom *Stephanodiscus*
740 *minutululus* (Bacillariophyceae). *J. Phycol.* 36, 510–522.

741 Martin, P., Lampitt, R.S., Jane Perry, M., Sanders, R., Lee, C., D’Asaro, E., 2011. Export and
742 mesopelagic particle flux during a North Atlantic spring diatom bloom. *Deep-Sea Res.*
743 PT I 58, 338–349.

744 Martin-Jézéquel, V., 1992. Effect of Si-status on diel variation of intracellular free amino
745 acids in *Thalassiosira weissflogii* under low-light intensity. *Hydrobiologia* 238, 159–167.

746 Martin-Jézéquel, V., Hildebrand, M., Brzezinski, M.A., 2000. Silicon metabolism in diatoms :
747 implications for growth. *J. Phycol.* 36, 821–840.

748 Mock, T., Samanta, M.P., Iverson, V., Berthiaume, C., Robison, M., Holtermann, K., Durkin,
749 C., Bondurant, S.S., Richmond, K., Rodesch, M., Kallas, T., Huttlin, E.L., Cerrina, F.,
750 Sussman, M.R., Armbrust, E.V., 2008. Whole-genome expression profiling of the marine
751 diatom *Thalassiosira pseudonana* identifies genes involved in silicon bioprocesses. *P.*
752 *Natl. Acad. Sci. USA* 105, 1579–84.

753 Moore, J.K., Doney, S.C., Glover, D.M., Fung, I.Y., 2002. Iron cycling and nutrient-
754 limitation patterns in surface waters of the World Ocean. *Deep-Sea Res. PT II* 49, 463–
755 507.

756 Moriceau, B., Garvey, M., Ragueneau, O., Passow, U., 2007. Evidence for reduced biogenic
757 silica dissolution rates in diatom aggregates. *Mar. Ecol. Prog. Ser.* 333, 129–142.

758 Moriceau, B., Goutx, M., Guigue, C., Lee, C., Armstrong, R.A., Duflos, M., Tamburini, C.,
759 Charrière, B., Ragueneau, O., 2009. Si–C interactions during degradation of the diatom
760 *Skeletonema marinoi*. *Deep-Sea Res. PT II* 56, 1381–1395.

761 Myklestad, S.M., 1995. Release of extracellular products by phytoplankton with special
762 emphasis on polysaccharides. *Sci. Total Env.* 165, 155–164.

763 Nelson, D.M., Tréguer, P., Brzezinski, M.A., Leynaert, A., Quéguiner, B., 1995. Production
764 and dissolution of biogenic silica in the ocean : Revised global estimates , comparison

765 with regional data and relationship to biogenic sedimentation. *Global Biogeochem. Cy.*
766 9, 359–372.

767 Nieuwenhuize, J., Maas, Y.E.M., Middelburg, J.J., 1994. Rapid analysis of organic carbon
768 and nitrogen in particulate materials. *Mar. Chem.* 45, 217–224.

769 Palmucci, M., Ratti, S., Giordano, M., 2011. Ecological and evolutionary implications of
770 carbon allocation in marine phytoplankton as a function of nitrogen availability: a fourier
771 transform infrared spectroscopy approach. *J. Phycol.* 47, 313–323.

772 Panagiotopoulos, C., Sempéré, R., 2005a. The molecular distribution of combined aldoses in
773 sinking particles in various oceanic conditions. *Mar. Chem.* 95, 31–49.

774 Panagiotopoulos, C., Sempéré, R., 2005b. Analytical methods for the determination of sugars
775 in marine samples : A historical perspective and future directions. *Limnol. Oceanogr.*
776 3,419-454.

777 Panagiotopoulos, C., Sempéré, R., 2007. Sugar dynamics in large particles during in vitro
778 incubation experiments. *Mar. Ecol. Prog. Ser.* 330, 67–74.

779 Panagiotopoulos, C., Sempéré, R., Obernosterer, I., Striby, L., Goutx, M., Van Wambeke, F.,
780 Gautier, S., Lafont, R., 2002. Bacterial degradation of large particles in the southern
781 Indian Ocean using in vitro incubation experiments. *Org. Geochem.* 33, 985–1000.

782 Panagiotopoulos, C., Sempéré, R., Para, J., Raimbault, P., Rabouille, C., Charrière, B., 2012.
783 The composition and flux of particulate and dissolved carbohydrates from the Rhone
784 River into the Mediterranean Sea. *Biogeosciences* 9, 1827–1844.

785 Panagiotopoulos, C., Wurl, O., 2009. Spectrophotometric and chromatographic analysis of
786 carbohydrates in marine samples. In: Wurl, O. (Ed.), Practical Guidelines for the
787 Analysis of Seawater. Taylor and Francis, pp. 49–65.

788 R Core Team, 2012. R: A language and environment for statistical computing. R Foundation
789 for Statistical Computing, Vienna, Austria.

790 Richardson, T.L., Cullen, J.J., 1995. Changes in buoyancy and chemical composition during
791 growth of a coastal marine diatom: Ecological and biogeochemical consequences. Mar.
792 Ecol. Prog. Ser. 128, 77–90.

793 Sarthou, G., Timmermans, K.R., Blain, S., Tréguer, P., 2005. Growth physiology and fate of
794 diatoms in the ocean: a review. J. Sea Res. 53, 25–42.

795 Shifrin, N.S., Chisholm, S.W., 1981. Phytoplankton lipids interspecific differences and effects
796 of nitrate, silicate and light-dark cycles. J. Phycol. 17, 374-384.

797 Smetacek, V., 1985. Role of sinking in diatom life-history cycles: ecological, evolutionary
798 and geological significance. Mar. Biol. 84, 239–251.

799 Soler, C., 2010. Impact des conditions de croissance sur le métabolisme et les interactions Si-
800 OC des diatomées - conséquences sur la vitesse de reminéralisation de la silice biogène
801 et de la matière organique. Ph.D. Thesis, Université de Bretagne Occidentale, France, pp
802 207.

803 Sorhannus, U., Ortiz, J.D., Wolf, M., Fox, M.G., 2010. Microevolution and speciation in
804 *Thalassiosira weissflogii* (Bacillariophyta). Protist 161, 237–49.

805 Størseth, T.R., Hansen, K., Reitan, K.I., Skjermo, J., 2005. Structural characterization of β -D-
806 (1 \rightarrow 3)-glucans from different growth phases of the marine diatoms *Chaetoceros mulleri*
807 and *Thalassiosira weissflogii*. *Carbohyd. Res.* 340, 1159–64.

808 Suroy, M., Boutorh, J., Moriceau, B., Goutx, M., 2014. Fatty acids associated to frustule of
809 diatoms and their fate during degradation – a case study in *Thalassiosira weissflogii*.
810 *Deep-Sea Res. PT I* 86, 21-31.

811 Tamburini, C., Garcin, J., Grégori, G., Leblanc, K., Rimmelin, P., Kirchman, D.L., 2006.
812 Pressure effects on surface Mediterranean prokaryotes and biogenic silica dissolution
813 during a diatom sinking experiment. *Aquat. Microb. Ecol.* 43, 267–276.

814 Tesson, B., Hildebrand, M., 2013. Characterization and localization of insoluble organic
815 matrices associated with diatom cell walls: Insight into their roles during cell wall
816 formation. *PLoS ONE* 8(4): e61675. doi:10.1371/journal.pone.0061675.

817 Thornton, D.C.O., 2002. Diatom aggregation in the sea: mechanisms and ecological
818 implications. *Eur. J. Phycol.* 37, 149–161.

819 Turley, C.M., Mackie, P.J., 1994. Biogeochemical significance of attached and free-living
820 bacteria and the flux of particles in the NE Atlantic Ocean. *Mar. Ecol. Prog. Ser.* 115,
821 191-203.

822 Turner, J.T., 2002. Zooplankton fecal pellets, marine snow and sinking phytoplankton
823 blooms. *Aquat. Microb. Ecol.* 27, 57–102.

824 Uitz, J., Claustre, H., Gentili, B., Stramski, D., 2010. Phytoplankton class-specific primary
825 production in the world's oceans: Seasonal and interannual variability from satellite
826 observations. *Global Biogeochem. Cy.* 24, GB3016, doi:10.1029/2009GB003680.

827 Urbani, R., Magaletti, E., Sist, P., Cicero, A.M., 2005. Extracellular carbohydrates released by
828 the marine diatoms *Cylindrotheca closterium*, *Thalassiosira pseudonana* and
829 *Skeletonema costatum*: effect of P-depletion and growth status. *Sci. Total Env.* 353,
830 300–306.

831 Velji, M.I., Albright, L.J., 1986. Microscopic enumeration of attached marine bacteria of
832 seawater, marine sediment, fecal matter, and kelp blade samples following
833 pyrophosphate and ultrasound treatments. *Can. J. Microbiol.* 32 : 121-126.

834 Volk, T., Hoffert, M.I., 1985. Ocean carbon pumps: Analysis of relative strengths and
835 efficiencies in ocean-driven atmospheric CO₂ changes. In: Sunquist, E.T., Broecker,
836 W.S. (Eds.), *The Carbon Cycle and Atmospheric CO₂: Natural Variations Archean to*
837 *Present*. American Geophysical Union, Washington, DC, pp. 99–110.

838 Waite, A.M., Bienfang, P., Harrison, P.J., 1992. Spring bloom sedimentation in a sub-arctic
839 ecosystem.1. Nutrient sensitivity. *Mar. Biol.* 114, 119–129.

840 Walne, P.R., 1966. Experiments in the large scale culture of the larvae of *Ostrea edulis* L.
841 *Fishery Investigations, Series II XXV (4)* 52 pp.

842

843

844

845

846

847

848

849 *Figure Legends:*

850 **Figure 1.** Schematic presentation of the experimental design and sampling of TW cells.

851 **Figure 2.** Evolution of the prokaryotic concentrations over time in the ‘Nutrient-replete’, ‘N-
852 stress’, and ‘Si-stress’ batches during the biodegradation experiments. The prokaryotic
853 concentrations correspond to the sum of the free and attached prokaryotes. N = 1 at each
854 sampling point.

855 **Figure 3.** Time course responses of the (A) POC and (B) PON relative concentrations of TW
856 in the ‘Nutrient-replete’, ‘N-stress’, and ‘Si-stress’ batches. The relative concentrations were
857 calculated by dividing the concentration at day t by the concentration at day 1 for both POC
858 and PON. The POC and PON concentrations were corrected by the C- and N- content of the
859 attached prokaryotes (see section 2.3). The vertical lines in the graph show the substitution
860 time for the two pools of organic matter for each experiment (Table 3). Replicates (n = 3)
861 were performed at days 1, 5, 10, 15, 22, and 30 and were used to feed our degradation model
862 (section 2.5).

863 **Figure 4.** Time course responses of the PCHO-C relative concentrations in the ‘Nutrient-
864 replete’, ‘N-stress’, and ‘Si-stress’ batches. The relative concentrations were calculated by
865 dividing the concentration at day t by the averaged concentration at day 1. The kinetics were
866 estimated using equation (3) (section 2.5). We used the concentration measured on day 1 as
867 the initial concentration. All of the experimental points correspond to one measurement
868 except at day 1 and day 30 (n = 3).

869 **Figure 5.** Time course responses of (A) galactose, (B) ribose, and (C) glucose in the
870 ‘Nutrient-replete’, ‘N-stress’, and ‘Si-stress’ batches. The kinetics were estimated using
871 equation (3) (section 2.5) and the concentrations at day 1 as the initial concentrations. The
872 degradation rates for galactose (N-stress batch), ribose (Si-stress batch), and glucose (Si-stress
873 batch) were no significant at the 0.05 level (see Table 3). All of the experimental points
874 correspond to one measurement except at day 1 and day 30 ($n = 3$).

875 **Figure 6.** Time course responses of the POC/PON ratio in the ‘Nutrient-replete’, ‘N-stress’,
876 and ‘Si-stress’ batches during the TW biodegradation. As in Figure 2, the vertical lines show
877 the substitution t_s time (see section 2.5) for the POC (bold) and PON (not bold) parameters.

878

879 Table 1. Initial parameters measured in each batch at the beginning of the experiment. The prokaryotic inoculum
 880 concentrations were estimated before the addition of the diatom cells.

Growth conditions	Batch volume (L)	[Diatom cells] (cell L ⁻¹)	Cellular volume ¹ (μm ³)	[POC] ² /[diatom cell] (pmol cell ⁻¹)	[PON] ² /[diatom cell] (pmol cell ⁻¹)	[Inoculum] (cell L ⁻¹)	[bSiO ₂]/[diatom cell] (pmol cell ⁻¹)
Nutrient- replete	10	1.80 x 10 ⁸	1488 ± 117	8.14	1.17	5.00 x10 ⁹	1.90
N- stress	10	3.02 x 10 ⁸	1154 ± 137	14.39	0.73	2.55x10 ⁹	0.89
Si- stress	10	2.11 x 10 ⁸	1364 ± 150	17.41	1.51	5.39x10 ⁹	0.86

881 ¹Cellular volumes were calculated at the end of the starvation experiment.

882 ²POC and PON values were corrected from the carbon and nitrogen contributions of the attached prokaryotes, respectively (see section 2.3).

883
 884
 885
 886
 887
 888
 889
 890
 891
 892
 893
 894
 895
 896
 897
 898
 899
 900
 901
 902
 903
 904

905 Table 2. Elemental carbohydrate compositions (percentage of the total sugar, mol%) and the total PCHO-C
 906 concentrations (in μM) during the 30 days of the degradation. The PCHO yields are given as the percentage
 907 of total PCHO-C to the POC. Abbreviations: Fuc. – Fucose; Rha. – Rhamnose; Ara. – Arabinose; GlcN. –
 908 Glucosamine; Gal. – Galactose; Glc. - Glucose; Man. – Mannose; Xyl. – Xylose; Rib. – Ribose; GalUA. –
 909 Galacturonic Acid. The values given at day 1 and 30 are the mean of three measurements (see Fig. 3).

Experiment	Time (d)	Fuc.	Rha.	Ara.	GlcN.	Gal.	Glc.	Man.	Xyl.	Rib.	GalUA	PCHO-C	PCHO-C/POC
Nutrient - replete	0	2.73	8.10	0.32	1.03	37.53	5.51	5.53	9.34	21.97	7.95	30.01	2.03
	1	2.57	8.04	0.19	3.62	15.04	8.36	4.27	6.47	46.69	4.75	102.55	5.22
	6	4.78	15.19	1.02	4.99	15.37	9.55	9.95	13.29	16.97	8.89	85.99	8.06
	12	6.80	14.26	3.37	4.83	13.28	8.86	9.16	11.97	16.04	11.42	41.90	6.59
	25	7.07	13.59	1.86	7.06	13.11	11.78	9.49	15.72	7.21	13.11	36.74	7.66
	30	8.28	12.69	2.33	6.74	12.53	13.47	8.35	16.79	6.71	12.10	30.64	6.26
N-stress	0	5.37	7.98	0.29	1.30	28.59	32.43	6.29	13.04	3.54	1.18	77.77	1.75
	1	2.45	6.36	0.32	1.81	11.82	43.02	3.65	7.33	22.87	0.37	193.95	4.02
	6	4.16	10.91	0.36	3.52	12.76	28.53	7.57	10.52	20.13	1.56	164.45	4.97
	12	5.29	12.76	1.11	4.89	14.40	22.28	10.22	14.12	12.74	2.20	145.90	7.94
	18	5.56	12.50	1.18	5.04	15.09	24.50	10.83	13.29	9.34	2.67	108.54	6.39
	25	5.21	7.74	0.28	1.26	27.74	31.47	6.10	12.66	3.43	4.12	94.25	6.90
30	7.67	11.17	2.20	4.81	13.54	25.40	9.08	14.27	9.85	2.00	60.65	4.26	
Si-stress	0	4.10	11.38	0.30	2.01	37.62	5.20	8.13	18.65	10.56	2.04	114.93	3.05
	1	3.38	11.61	0.22	4.12	17.66	12.14	4.77	11.64	34.06	0.40	162.92	3.84
	6	3.23	12.11	0.23	5.13	8.14	19.72	5.00	9.67	36.77	0.00	219.95	6.78
	12	6.27	16.57	1.24	5.93	10.97	13.80	9.91	16.98	18.33	0.00	87.36	5.23
	18	7.15	16.22	1.57	7.41	11.89	13.53	11.82	17.91	12.50	0.00	57.51	3.54
	30	7.26	16.26	3.06	7.17	11.66	15.83	10.85	18.68	9.23	0.00	68.06	5.18

910

911 Table 3. Estimated kinetic parameters for POC, PON, PCHO, and the individual monosaccharides (see equations in section
 912 2.5) during degradation of TW. The t_s value is the substitution time between the two pools of organic matter. The standard
 913 error (SE) is given for each estimation. Significant estimations are underlined ($p < 0.05$).

Kinetic parameters	Nutrient-replete						N-stress						Si-stress					
	k_1		k_2		t_s		k_1		k_2		t_s		k_1		k_2		t_s	
	Value	SE	Value	SE	Value	SE	Value	SE	Value	SE	Value	SE	Value	SE	Value	SE	Value	SE
POC (n=34)	<u>0.111</u>	0.031	<u>0.04</u>	0.001	<u>5.908</u>	0.561	<u>0.096</u>	0.002	<u>0.018</u>	0.001	<u>11.14</u>	0.181	<u>0.113</u>	0.005	<u>0.014</u>	0.001	<u>8.544</u>	0.237
PON (n=34)	<u>0.191</u>	0.099	<u>0.054</u>	0.001	<u>4.989</u>	0.587	<u>0.044</u>	0.002	<u>0.021</u>	0.001	<u>10.54</u>	0.639	<u>0.078</u>	0.002	<u>0.019</u>	0.001	<u>10.07</u>	0.127
Kinetic parameters	k (n = 9)						k (n = 10)						k (n = 9)					
	Value		SE				Value		SE				Value		SE			
Fuc.	0.004		0.01				0.002		0.006				0.005		0.005			
Rha.	0.027		0.011				0.017		0.01				<u>0.022</u>		0.009			
Ara.	-0.014		0.019				-0.015		0.016				<u>-0.057</u>		0.009			
GlcN.	0.022		0.01				0.01		0.013				0.014		0.01			
Gal.	<u>0.054</u>		0.01				0.018		0.009				<u>0.06</u>		0.018			
Glc.	<u>0.028</u>		0.01				0.071		0.037				0.029		0.02			
Man.	0.021		0.013				0.009		0.012				0.004		0.007			
Xyl.	0.012		0.011				0.012		0.007				0.016		0.007			
Rib.	<u>0.215</u>		0.054				<u>0.050</u>		0.007				0.073		0.043			
GalUA	0.009		0.009				-0.01		0.019				-		-			
Total PCHO	<u>0.046</u>		0.01				<u>0.036</u>		0.009				<u>0.036</u>		0.014			

914

915

916

Figure

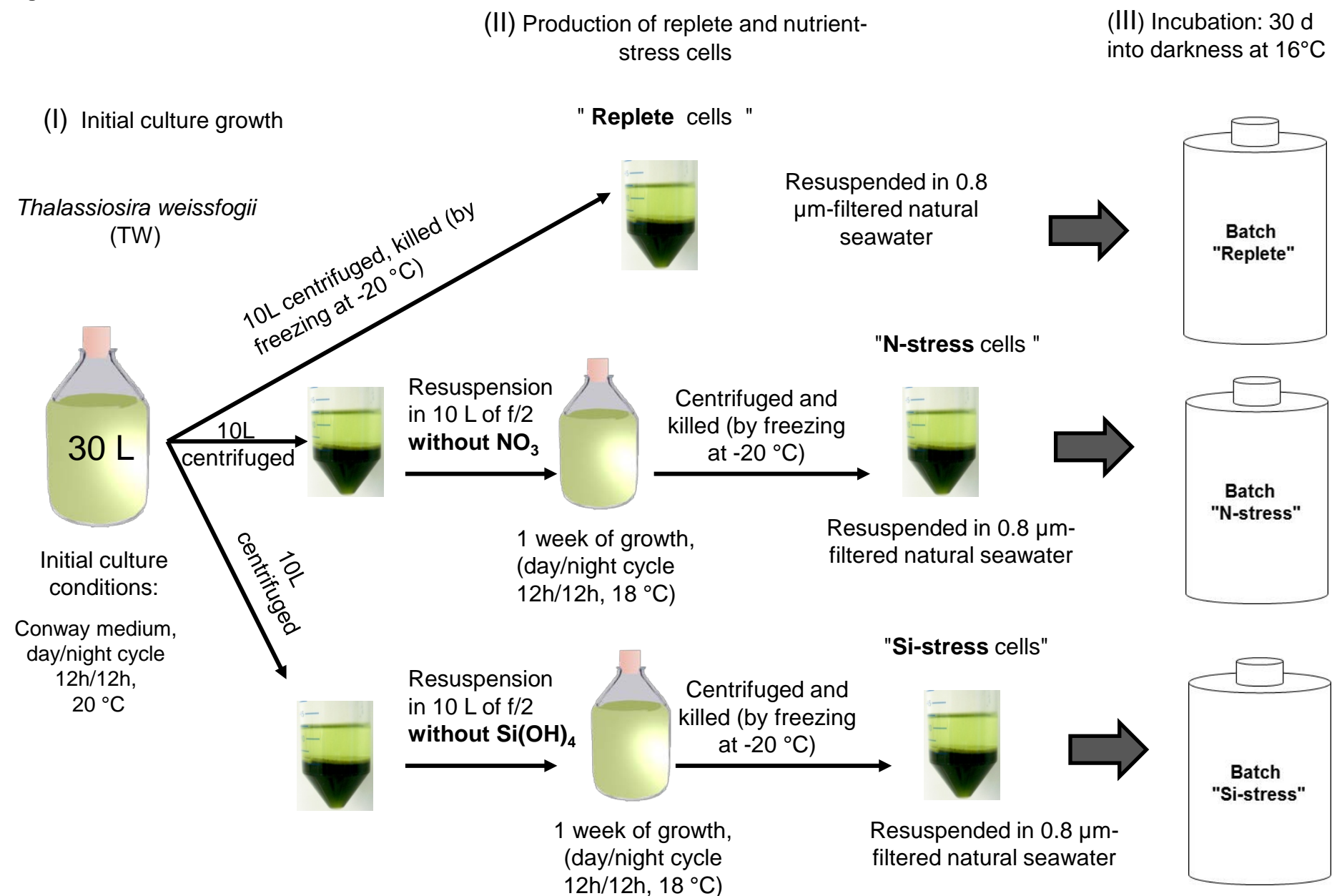


Figure 1

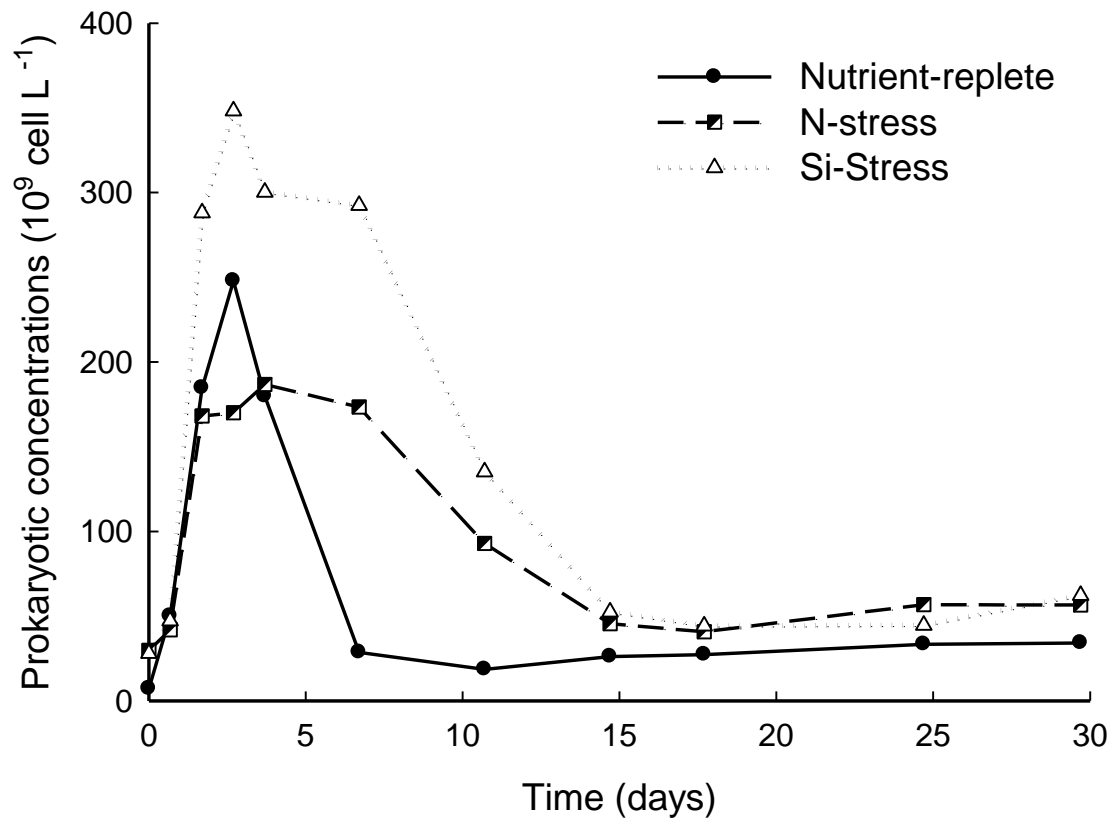


Figure 2

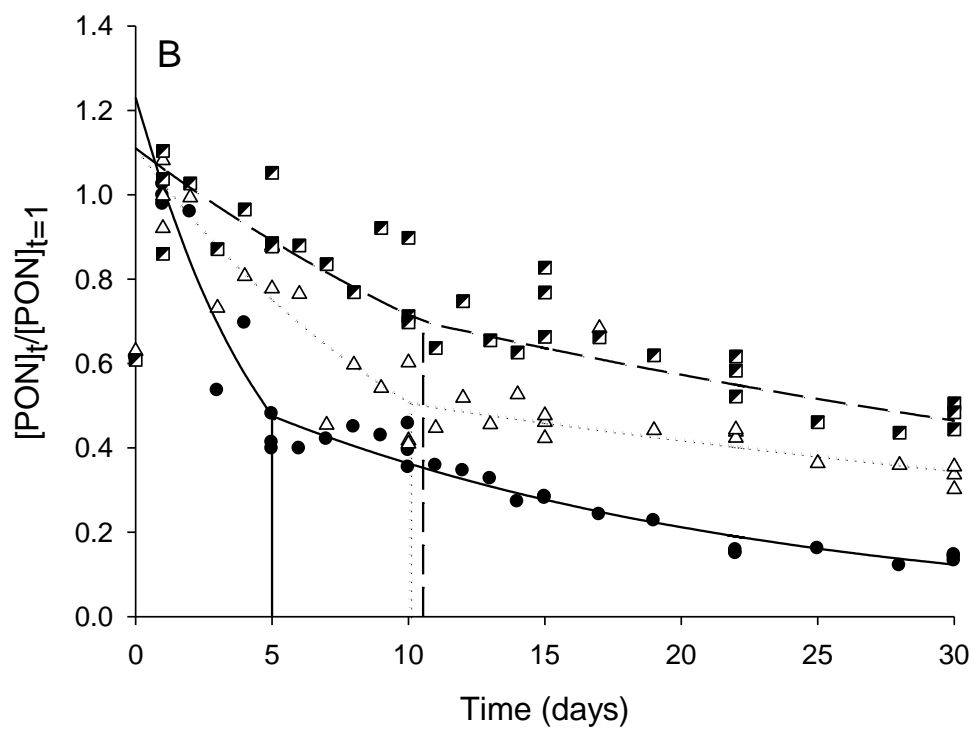
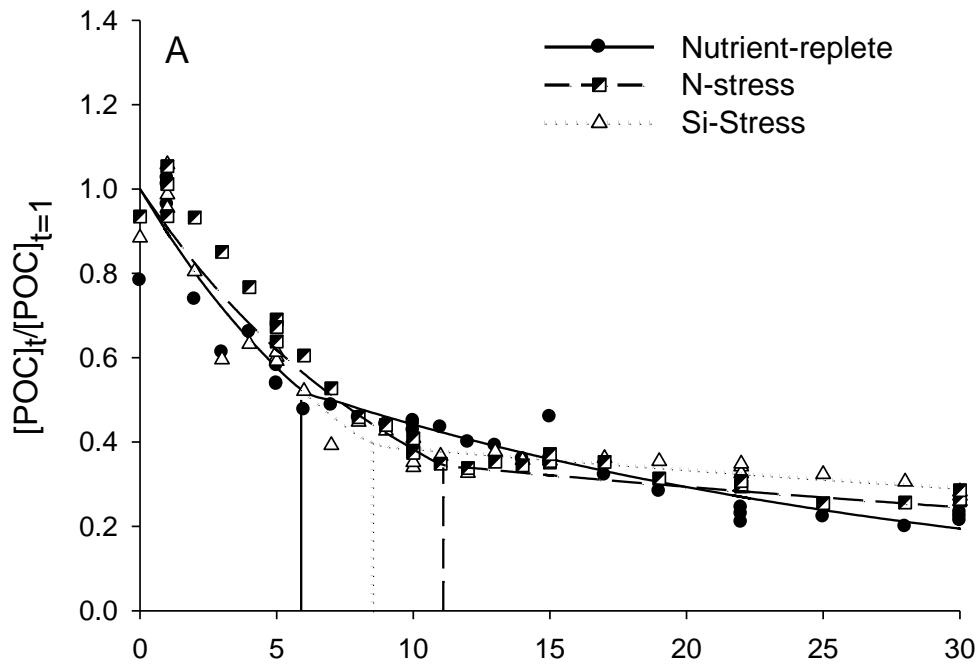


Figure 3

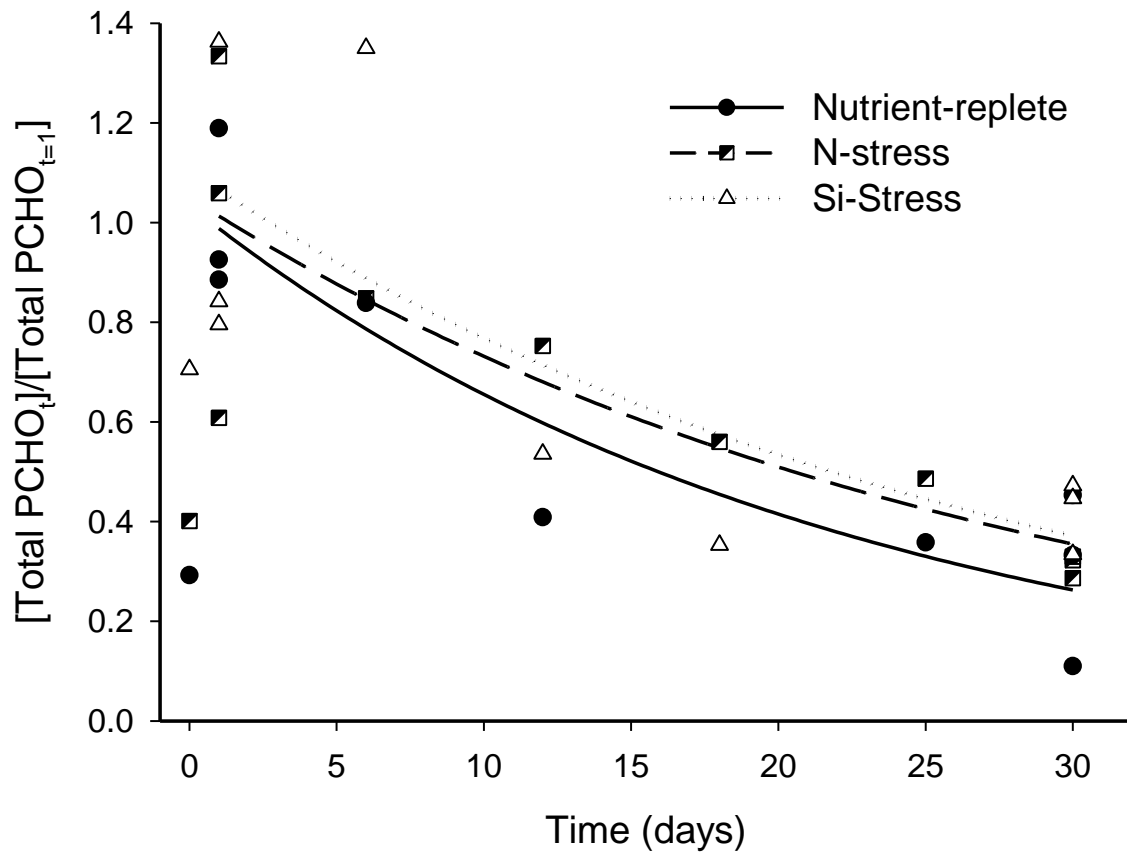


Figure 4

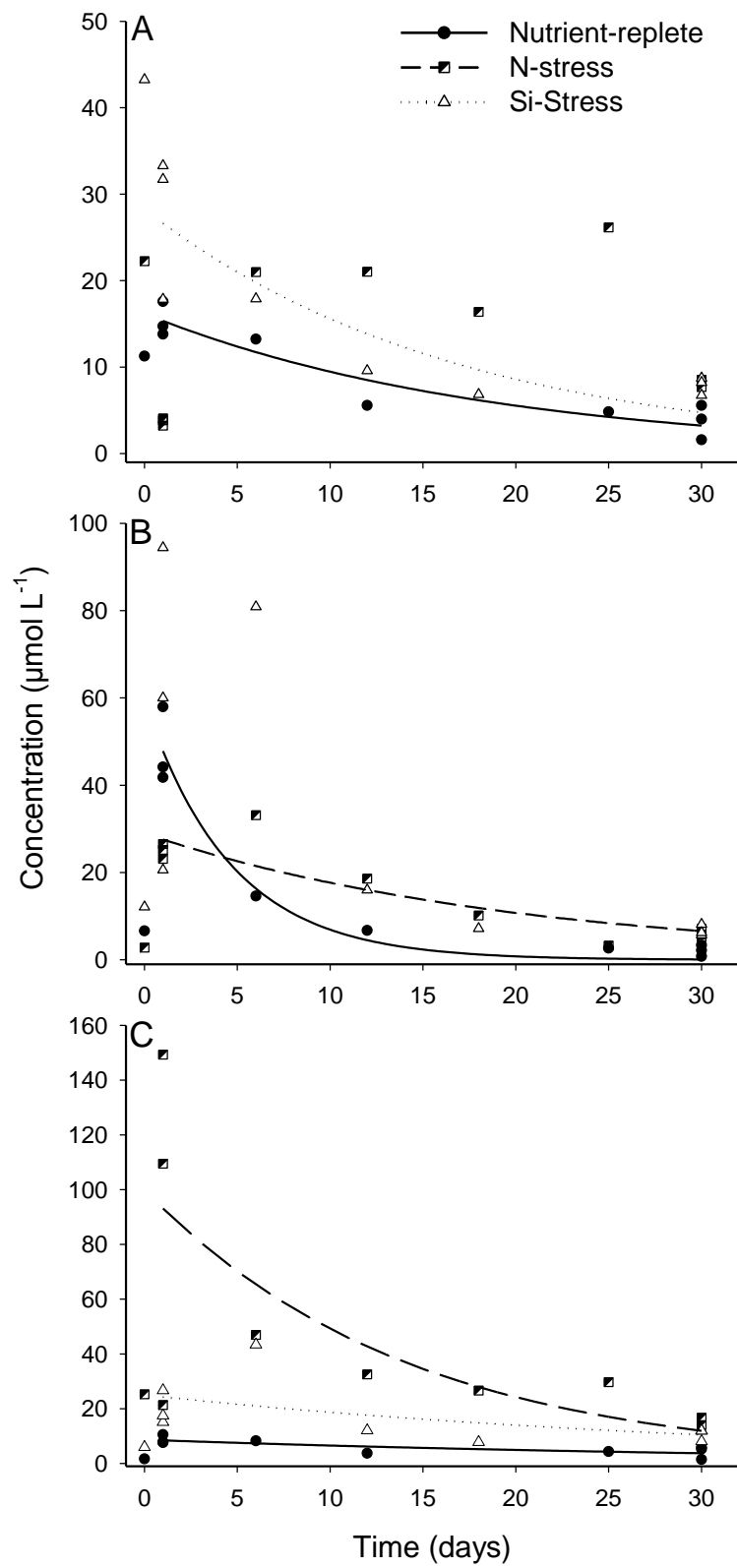


Figure 5

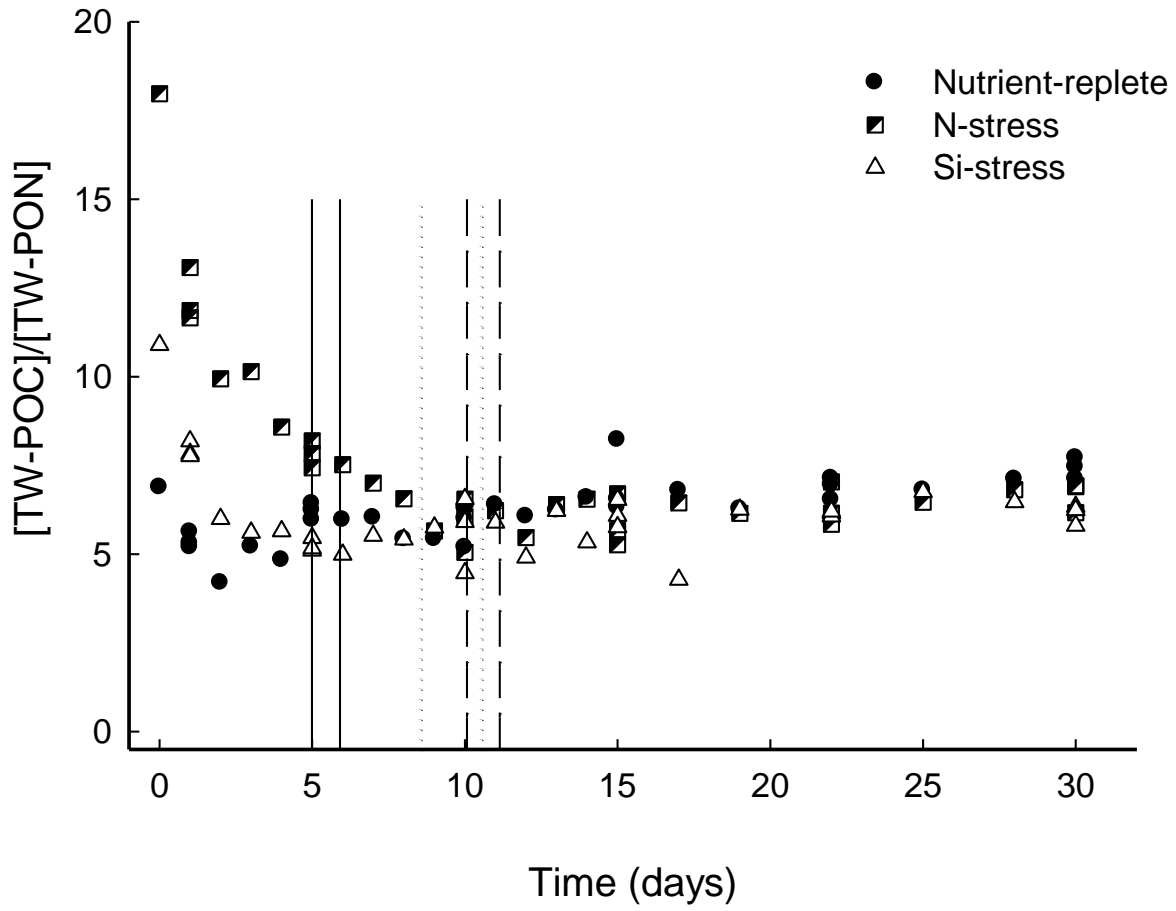


Figure 6